IEEE Access
Multidisciplinary | Rapid Review | Open Access Journal

Received September 18, 2020, accepted October 26, 2020, date of publication November 5, 2020,
date of current version November 18, 2020.

Digital Object Identifier 10.1109/ACCESS.2020.3036133

Optimization Design of Self-Triggered Complex Detector for Space Range-Gated Imaging System

YINING MU[1], FANQI TANG[1], MAKRAM IBRAHIM[2], YAN ZHU[1], WENXIN LIU[1], ZHE CAO[1], AND TIANQI CHEN[1]

[1]Faculty of Science, Changchun University of Science and Technology, Changchun 130022, China
[2]National Research Institute of Astronomy and Geophysics, Cairo 11421, Egypt

Corresponding author: Yining Mu (muyining1985@hotmail.com)

This work was supported in part by the National Natural Science Foundation of China under Grant 51602028, Grant 61905026, and Grant 11874091; in part by the Jilin Province Science and Technology Development Project under Grant 20200301065RQ and Grant 20190701024GH; and in part by the Chinese Academy of Sciences under Grant CAS- KLAOT-KF201803.

ABSTRACT To further enhance transient characteristics of space range-gated imaging system and widen its application potential in astronomical and military domains, a self-triggered structure and complex detecting mechanism are proposed in this paper. There being delays restriction among multiple subsystem of range-gated imaging system and the robust performance of multiple optical axis adjusted are firstly discussed and analyzed. Based on these, by researching the work principle and coupling process of microchannel plates in series in image intensifier, taking advantages of the coupling loss electrons to realize self-triggered is studied and its prototype device structure is further proposed too. Then, the space optical transfer theory of new self-triggered component is deduced and its waveguide process is simulated in the software. Finally, the self-trigger performance and optical transfer effect of cutting edge invention is verified by vacuum test. And the test results basically match with theoretical model and simulation data.

INDEX TERMS Micro channel plate (MCP), range- gated imaging, self- triggered, complex detector.

I. INTRODUCTION

In recent years, as an advanced imaging technology with distinguished signal-to-noise ratio (SNR) and transient detecting ability, active range-gated imaging has been widely studied and applied in space awareness and military field [1]–[5]. Thanks to the rapid progress of laser and optics technology and imaging detector, some performances of range-gated imaging have made great improvements, especially the time resolution of some subsystems or components have reached the nanosecond level [6]–[9]. However, in practical applications, many delays between each subsystems or components have created a critical barrier to further enhancements of time resolution to transient imaging [10]–[12]. Namely, it is extremely difficult for multiple subsystems to realize a synchronization trigger at the nanosecond level in the range-gated imaging process, which directly limits further progress of the overall system [13]–[16]. Therefore, it is very worthwhile to reduce or cancel the series delays in range-gated imaging system [17]–[19].

The associate editor coordinating the review of this manuscript and approving it for publication was Bora Onat.

On the other hand, in order to receive more echo optical power from space, larger and larger aperture of optical antenna never fails to fascinate designer of space optoelectronic system. But, excessive aperture will directly cause longer focal length for ensuring quality of imaging. As key triggered component, avalanche photodiode (APD) is field stop of traditional range-gated imaging system. Meanwhile, in order to ensure transient trigger of range-gated imaging, the photo surface of APD is not too large, generally is sub-millimeter scale. Therefore, the field of view (FOV) is usually greatly limited by the excessive aperture and minute FOV. In the micro-assembly process of range-gated imaging system, there is a precise adjusting step between echo trigger and laser emitting optical axis. Visibly, the precise adjusting of multiple optical axis can not only greatly limit its FOV and flexibility of space range-gated imaging, but also obviously enhance the risk of off-axis and reduce the reliability of range-gated imaging system in the space.

To address above both issues, a complex detecting device mechanism is proposed in this paper. We took advantages of coupling loss electrons between the MCPs to self- triggered transient imaging, which will directly avoid the series delays

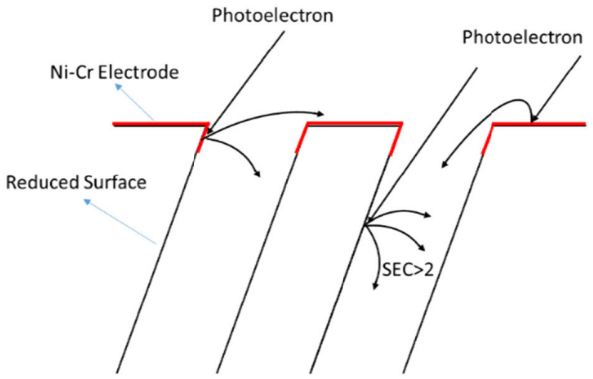

FIGURE 1. Coupling loss electron schematic diagram.

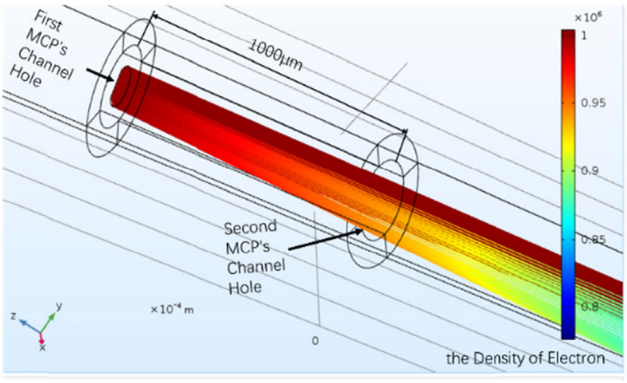

(a) There being 1000V between the lower surface and the upper surface of the MCPs

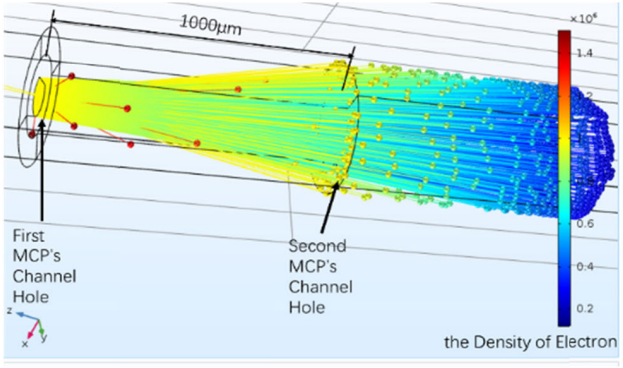

(b) There being 0V between the lower surface and the upper surface of the MCPs

FIGURE 2. Electron beam diffusion in coupling Process.

from every subsystem and immediately enhance transient characteristics of range-gated imaging system, but also make the echo trigger and range-gated imaging subsystem combine two into one, and effectively improve robustness of range-gated imaging system in tough environments.

II. SELF-TRIGGERED MECHANISM

As the core component of range-gated imaging system, image intensifier provides the vast majority of amplification and gain of transient imaging [20], [21]. Therein, microchannel plate (MCP) is a distinguished electric-vacuum amplification device whose gain can reach 10^5 and frequency response is close to sub-nanosecond. Usually, two microchannel plates in series were widely applied by image intensifier for enhancing the gain of transient imaging. However, upon the work principle of MCP, there being two Ni-Cr thin film electrodes on the both sides of MCP is indispensable for supplement and multiplication of the currents [22]–[25]. The device structure will immediately lead to electrons loss of compling between MCPs and obviously reduce the currents density received by the second MCP. As shown in Fig. 1.

Many of electron beams are collected by the Ni-Cr electrode at the input of the MCP. Theoretically, the coupling efficiency can be dominated by designing parameter of the waveguide structure MCPs such as electric field distribution and gap scale between MCPs [26]–[28]. For example, in the Fig.2, the proportion of coupling loss can be obviously altered by only selecting both extreme bias voltages in the same waveguide structure. Herewith, by precisely controlling parameters of the whole waveguide structure can directly affect the proportion of the coupling loss from 20% to 90%.

On the basis, this paper proposed that setting a micro array-holes waveguide gate between both MCPs to collect coupling loss for self-trigger or other complex detecting [29]–[31]. As shown in Fig. 3, compared with MCP, the micro array-holes waveguide gate can be regarded as a microchannel plate with lower aperture ratio, there being metal conductive layer attached in the inner wall of the holes and no multiplication. The array-holes can be manufactured by laser-engraved on a mica plate of 20 microns. And MCP_2 and the array hole can be installed together by physical proximity model. The concrete structure and working principle of the prototype device are shown in Fig.4. The X of $CsPbX_3$ in the Fig.3 can adopt Br. Generally the bandgap of $CsPbBr_3$ is around 2.26eV and its emitting wavelength concentrate upon Green color. Because a random lasing based on $CsPbBr_3$ pumped by high energy electric beam has been verified in our team other paper. So taking advantages of $CsPbBr_3$ can contribute to reduce noise from electric amplification. Its manufacturing method and process are as follows. The quantum dot spin coating solution obtained by one-step spin coating method is dropped on a conductive glass substrate through a special syringe. Finally, spin coating resulted in a uniformly translucent $CsPbBr_3$ quantum dot film. Besides, the conductivity of the perovskite layer can be set around 7 s/m.

When the echo laser pulse is focused on the photocathode by the optical antenna, a number of photo electrons with space imaging information are triggered from the photocathode. Under external electronic field, the photoelectrons stimulated by the laser pulse will enter into the MCP_1 to complete itself multiplication and to shape electron beam including space imaging information. Subsequently, the EB will be divided into two by the micro array-holes waveguide gate. Therein, the majority of EB is collected by the metal conductive

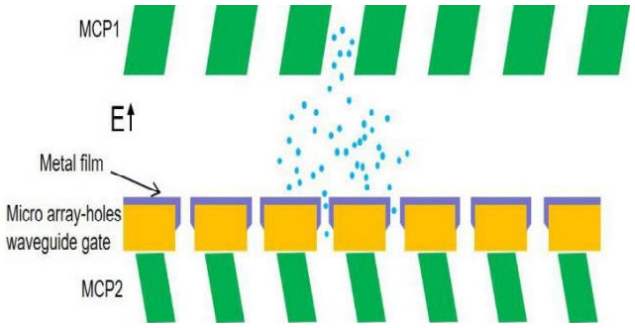

FIGURE 3. Micro array-hole waveguide grate mechanism.

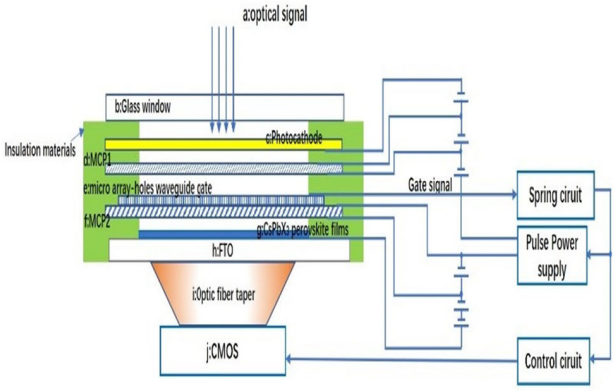

FIGURE 4. The prototype device structure and principle.

layer of micro array-holes waveguide gate during waveguide process, and the others of EB will pass through the micro array-holes waveguide gate and enter into the second MCP to recover the power of EB. The part collected by the metal conductive layer of EB is used for instantaneously triggered imaging and pulse power supply of MCP_2.The remaining part of EB amplified by the MCP_2 will transfer initial space imaging information to the final luminescent screen. Because of there being effect of self- saturated gain in multiple MCPs in series, collected EB's power from the coupling between MCPs will little affect the weak signal detection ability of overall device.

III. MODEL ANALYSIS AND SIMULATION

As shown in Fig. 4, theoretically, the overall resolution (S) of the image intensifier is mainly affected by the gap between photocathode and MCP_1, the distance between anode and MCP_2, and concrete structure parameters of micro array-holes waveguide gate, which is approximately expressed as:

$$\frac{1}{S^2} = \frac{1}{S_{\text{in}}^2} + \frac{2}{S_{\text{mcp}}^2} + \frac{1}{S_{\text{gate}}^2} + \frac{1}{S_{\text{out}}^2} \tag{1}$$

It is known that the molecule size of photocathode and anode are so minute sufficiently that the constraint of both portions can be neglected to overall resolution. Besides, thanks to great enhancement of MCP manufacturing technology, the hole scale of MCP has reached micron order. Upon the sampling theorem of MCP, its resolution can be expressed as:

$$S_{\text{mcp}} = \frac{1000}{\sqrt{3p}} \tag{2}$$

where the p represents the diameter of MCP's hole. Visibly, if the p is around several microns, the overall resolution (S) is little affected by the dimensions of MCP. However, in traditional image intensifier, the distance between MCP_2 and anode is mainly restricted factor. Because of there being external high voltage accelerates EB for the anode emitting light, the distance between MCP_2 and anode generally cannot too tiny, which will directly diffuse EB focal spot and lose space imaging information. Note that in traditional image intensifier, multiple MCPs generally take advantages of proximity focusing to install for reducing EB diffusion. But in order to add micro array-holes waveguide gate between MCPs, the gap taken by the micro array-holes waveguide gate will become a new avoidable bottleneck.

Resolution expression of the both parts can be approximately as the process of EB diffusion in vacuum. So their resolution expression can be written as:

$$S_{\text{out}} = 2\text{D}_{\text{out}}\sqrt{\frac{2\text{E}_x}{\text{qU}_{\text{out}}}} \tag{3}$$

$$S_{\text{gate}} = 2\text{D}_{\text{gate}}\sqrt{\frac{2\text{E}_x}{\text{qU}_{\text{gate}}}} \tag{4}$$

where the Ex represents the initial average kinetic energy of electron from MCP, and the D_{gate} and U_{gate} are respectively the gap and voltage between MCP_1 and micro array-holes waveguide gate, and the D_{out} and U_{out} are respectively the distance and the voltage between MCP_2 and anode. However, in the above formula, although the D_{gate} and D_{out} linearly affect relative resolution, and the U_{out} around several thousand voltages is generally far more than U_{gate} around several dozen voltages. Therefore, the S_{gate} is mainly and newly limited factor, and the structure parameters of micro array-holes waveguide gate should be optimized as much as possible.

Upon the optical imaging and estimate theory, space optical transfer characteristics of imaging system can be measured by normalizing the real part of the Fourier transform of point impulse function. Generally, modulation transfer function (MTF) represented by the real part of point impulse function can effectively show attenuation process space of frequency spectrum between object and image. On the basis. The optical transfer expression of the new image intensifier system can be simplified as follows.

$$\text{MTF} = \text{MTF}_{\text{in}} \times 2\text{MTF}_{\text{mcp}} \times \text{MTF}_{\text{gate}} \times MT\text{F}_{\text{out}} \tag{5}$$

The MTF of MCP can be given by equation 6, where p is the diameter of every micro hole and f is the space frequency of imaging and J_1 represents the first order Bessel function.

$$\text{MTF}_{\text{mcp}} = \left| \frac{\text{J}_1(2\pi f\text{p})}{\pi f\text{p}} \right| \tag{6}$$

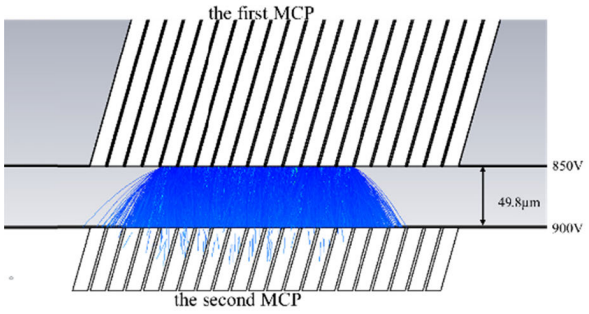

(a)Under the same voltage the excessive waveguide gap leads to uneven distribution of electric field

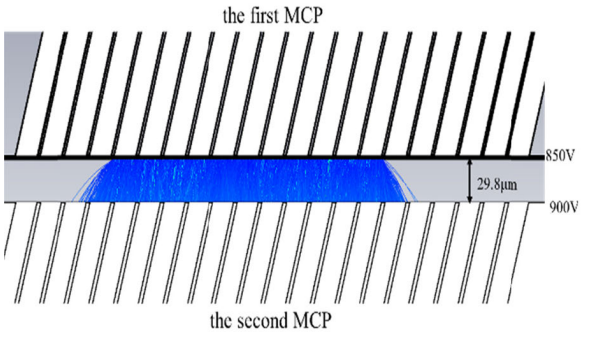

(b)Under the same voltage the distance between two MCPs is around 30 μm leads to reasonable electric field distribution

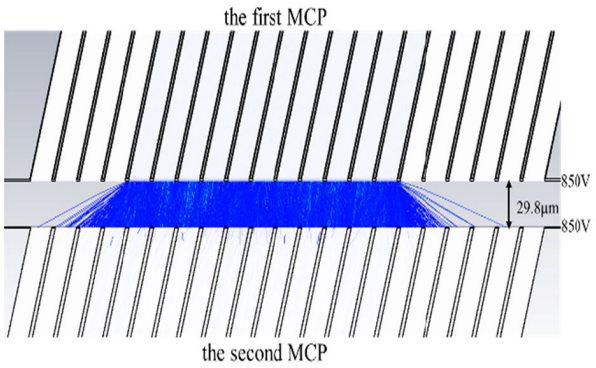

(c)Under the different voltage leads to lack of guide electric field

FIGURE 5. Difference of coupling loss.

The MTF of proximity cathode can be expressed as:

$$\mathrm{MTF_{in}} = \exp\left(-4\pi^2 \mathrm{D_{in}^2 f^2} \frac{E_{in}}{U_{in}}\right) \tag{7}$$

where D_{in} is proximity gap between cathode and MCP_1, and E_{in} is initial kinetic energy of electrons from cathode into vacuum, and the U_{in} is the voltage between MCP_1 and cathode.

Similarly, the MTF of anode and micro array-holes waveguide gate can be expressed as:

$$\mathrm{MTF_{anode}} = \exp\left(-\frac{\pi^2 D_{anode}^2 f^2 E_x}{9\mathrm{U_{out}^2}}\right) \tag{8}$$

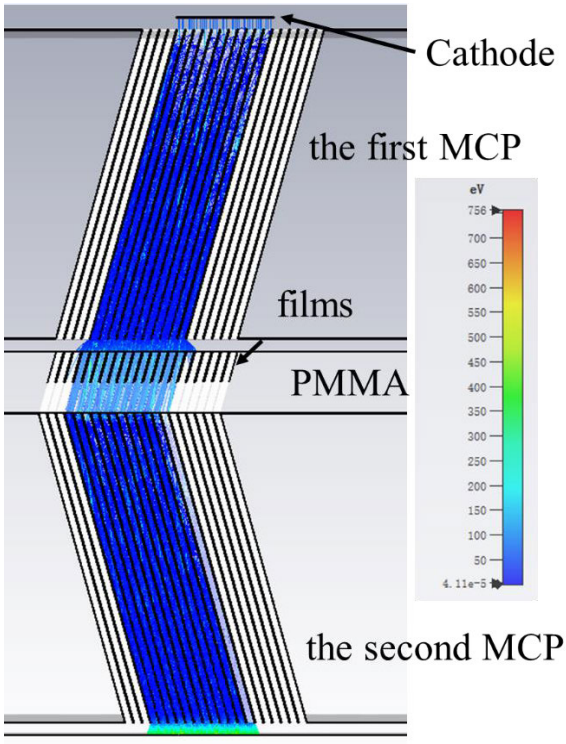

FIGURE 6. Integrated waveguide process.

$$\mathrm{MTF_{gate}} = \exp\left(-\frac{\pi^2 D_{gate}^2 f^2 E_x}{9\mathrm{U_{gate}^2}}\right) \tag{9}$$

By comparing with other sub MTF function expression, the MTF_{gate} plays the most important role in the overall MTF of the new-type image intensifier. Especially, the precise manufacturing and optimized designing of D_{gate} and U_{gate} are importance of final imaging. Visibly, provided the structure parameters of micro array-holes waveguide gate set reasonably, the initial EB imaging information is little affected by the diffusion of waveguide structure. And Fig.6 shows the overall waveguide process of Fig.5 .

In the system of Fig.6, we set several typical resolution patterns which are respectively 10lp/mm, 12.5lp/mm, 15lp/mm and 20lp/mm as imaging targets. After waveguide transfer, their corresponding patterns at image space can be showed in Fig. 7.

To sum up, upon theoretical analysis of from 6 to 9 formula, we fitted the theoretical optical transfer function of micro array-holes waveguide gate depending on simulating data, as shown in Fig.8. It is not difficult to find that the above several typical simulated patterns almost match with the theoretical optical transfer function. The space optical transfer ability of new device structure can satisfy practical application and additional self-triggered component basically does not affect imaging performance of overall image intensifier.

IV. MANUFACTURING AND TESTING

In order to further verify the above theoretical analysis and simulation results, we established a prototype device in the

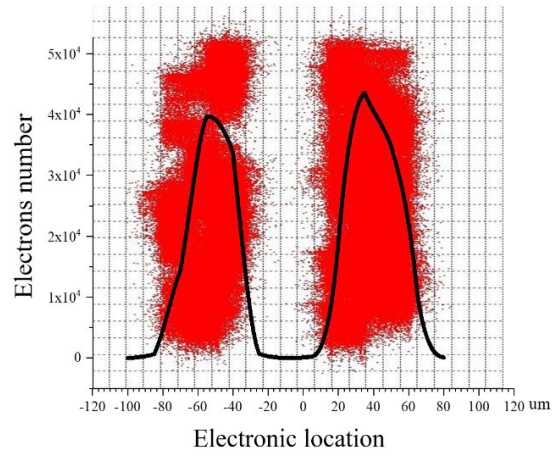

(a)10lp/mm Electric pattern at image space

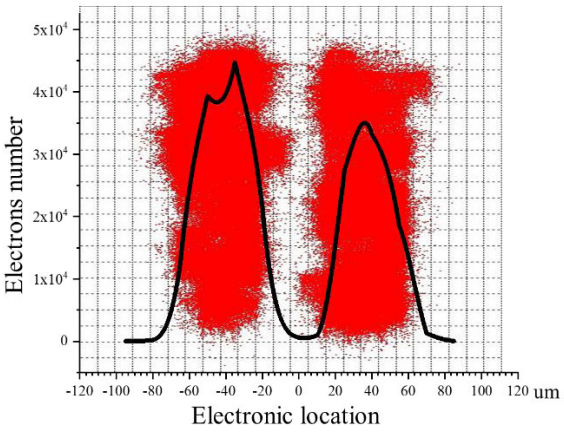

(b)12.5lp/mm Electric pattern at image space

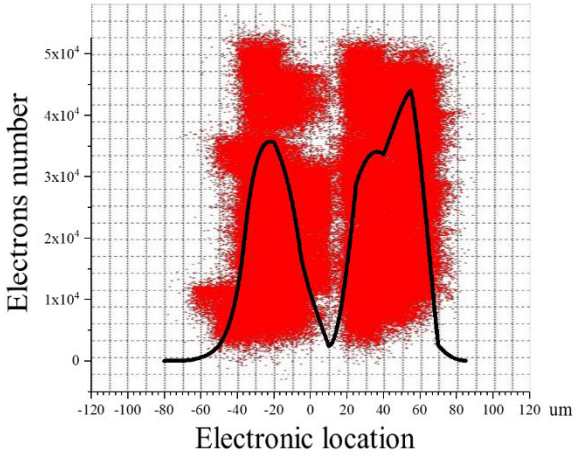

(c)15lp/mm Electric pattern at image space

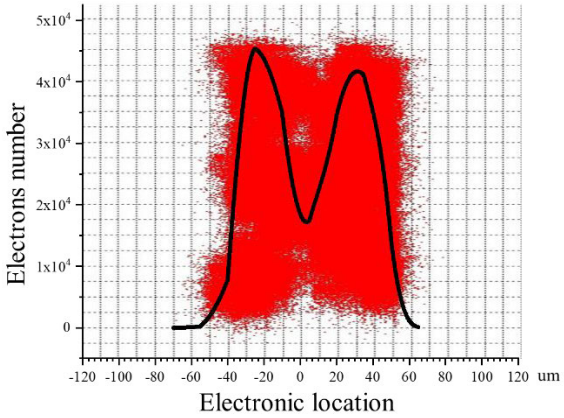

(d)20lp/mm Electric pattern at image space

FIGURE 7. Electric-optical space transfer effect.

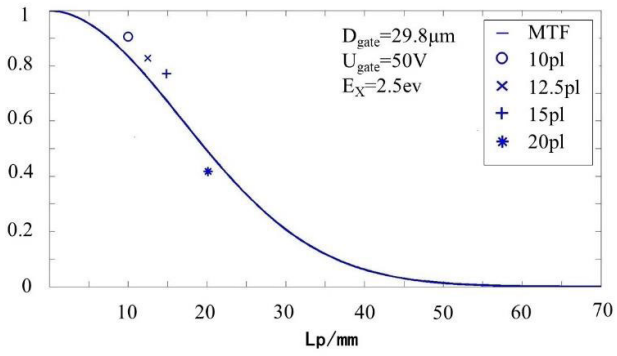

FIGURE 8. Optical transfer function.

vacuum in light of the Fig.4. The concrete manufacturing process and steps are as follows.

The first step, we took advantages of silicon slice as the substrate to manufacture micro array-holes waveguide gate. A massive of induced pits were etched in the silicon slice by inductively coupled plasma (ICP). The process and result of detailed manufacturing can be shown in Fig.9.

The second step, we made use of thermal evaporation to deposit Al film in and on the micro array-holes waveguide gate. Note that during process of the thermal evaporation deposition, there is a tiny angle of around degree between evaporation source turret and micro array-holes waveguide gate. The depth of the metal conductive layer in the micro array-holes can be further deepened by the smaller angle, which also enhance the resistivity of the gate films. The characterization of plane surface is showed in the Fig.10. Visibly, there is a metal conductive layer film of around 337nm on the surface of micro array-holes waveguide gate sample. On the other hands, because the thickness of metal conductive layer film on the inner wall of micro array-holes is gradually varied, the thickness and depth of metal conductive layer film on the inner wall is very difficult to exactly measure. But in Fig.10 (a), it is not difficult to find that at least 30% of the inner walls have been covered by the metal conductive layer film, which

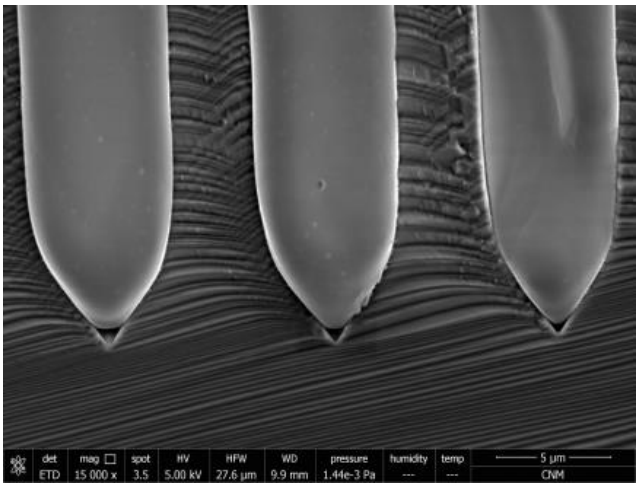

(a)Manufacturing process of induced pits

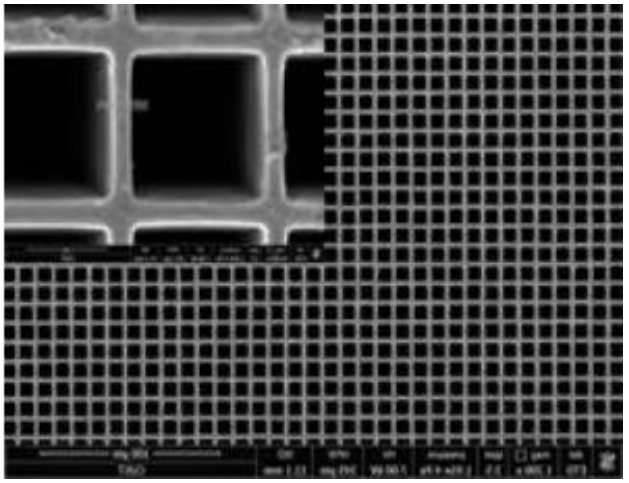

(a)Manufacturing result of micro array-holes

FIGURE 9. Substrate manufacturing.

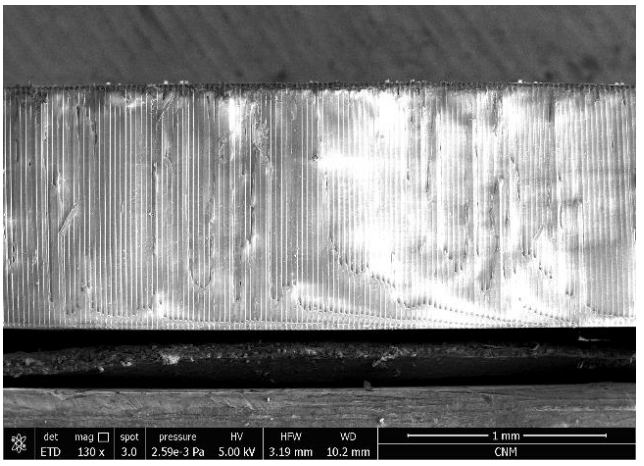

(a)Macroscopic Characterization Plane Effect

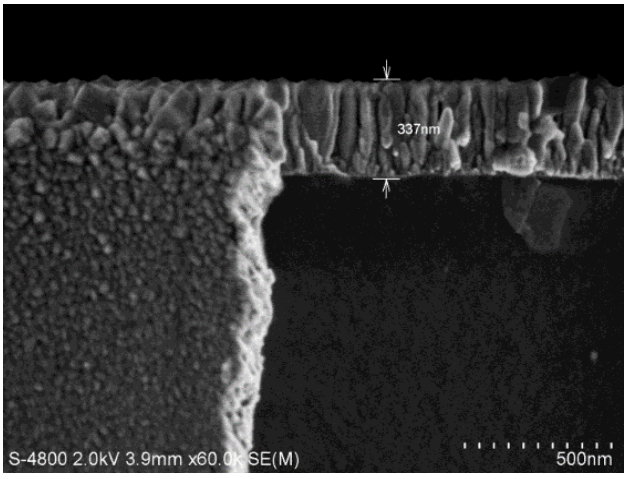

(b)Microscopic Characterization Plane Effect

FIGURE 10. Manufacturing characterization.

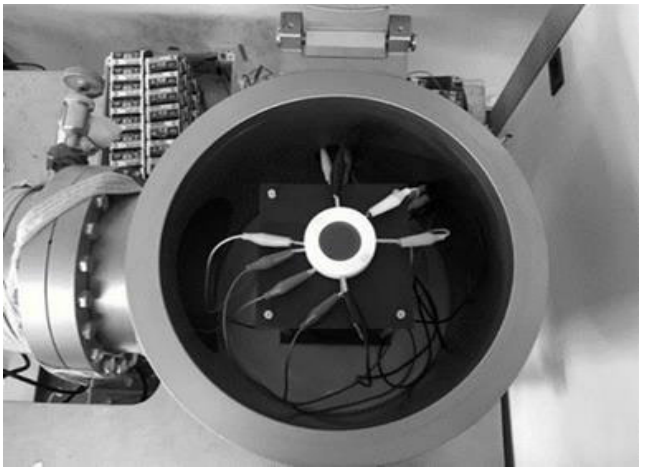

FIGURE 11. Prototype verification system.

already can estimate the above cutting-edge self-triggered model qualitatively.

Thirdly, in the prototype device, Au film was used as photocathode and it was triggered by an UV LED. The integrated effect of prototype device is shown in Fig.11.

The gap between the MCP_1 and the micro array-holes waveguide gate is restricted by a mica spacer of 30μm. EB allocation and waveguide process simulated by Fig.5 and 6 are verified and tested. In other words, the variation of gate and anode received EB are recorded by changing the electric field distribution between MCP_1 and the micro array-holes waveguide gate. Some tendency of these data basically match with the simulation of Fig.5 and 6. The concrete allocation relationship and testing results are shown in Fig.12. For example, the Fig.5 showed several distribution statuses of electric beam during extreme conditions. The Fig.6 showed a normal divided process of electric beam in the whole waveguide structure. Therefore, whether it is extreme status, or normal divided process, the Fig.12 include all above status. Namely, the data of Fig.12 reflected that electric beam divided and renewable process, which can verify possibility of achieving self-trigger in terms of device designing.

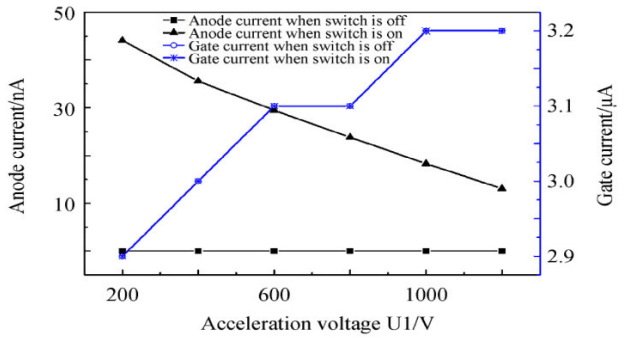

FIGURE 12. Self-trigger allocation relationship.

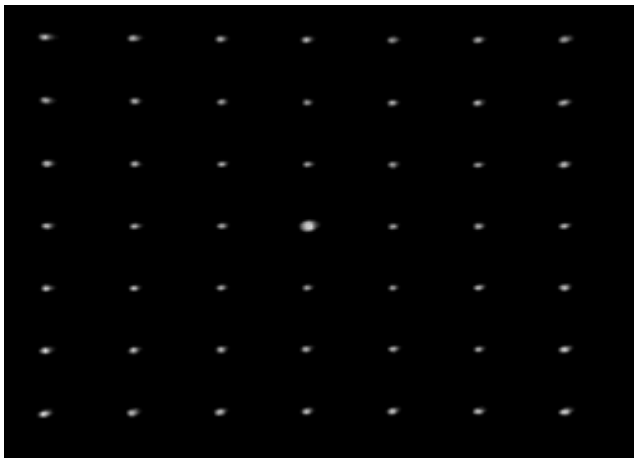

FIGURE 13. Finally imaging effect on standardized array-holes.

Of course, the concrete designing of self-trigger imaging system is also very important.

Finally, in order to verify that additional self-triggered device structure does affect initial resolution, standardized array-holes are set on the photocathode surface. There is no obviously optical distortion between object and imaging in the Fig.13.

V. CONCLUSION

In this paper, a cutting edge self-trigger detecting mechanism in image intensifier is proposed. This paper firstly researched and analyzed theoretical model and optimized designing method of the new detector. Secondly, in terms of simulation, its waveguide process and work principles were emulated in the CST. Finally, by vacuum test, its self-trigger and space optical transfer ability are verified, and its experiment results basically match with the theoretical analysis and the emulation model. Currently, according to reference of this paper, the time resolution of mainstream range gating imaging systems is only able to achieve several dozen microseconds. Upon our simulation results in the software, the self-trigger device structure can achieve management of electric beam in several dozen picoseconds level. We will integrate the self-trigger device and follow up to report its device characteristics and system advantages in the next paper. We think that the time resolution of self-trigger device maybe reaches several hundred nanoseconds at least.

To sum up, if this cutting edge invention proposed in this paper would be widely applied in image intensifier, space range-gated imaging system could have a more extensive application and technology upgrading potential in astronomical and military domains.

REFERENCES

[1] M. Xie, C. Ma, K. Liu, P. Liu, W. Hao, J. Han, W. Huang, X. Lian, X. Feng, and F. Jing, "The application of active polarization imaging technology of the vehicle theodolite," *Opt. Commun.*, vol. 433, pp. 74–80, Feb. 2019.

[2] Y. Lutz, E. Bacher, and S. Schertzer, "Accumulation mode laser range-gated viewing in the eye-safe spectral region," *Opt. Laser Technol.*, vol. 04, no. 96, pp. 1–6, Apr. 2017.

[3] Z. Chen, R. Fan, X. Li, Z. Dong, Z. Zhou, G. Ye, and D. Chen, "Accuracy improvement of imaging lidar based on time-correlated single-photon counting using three laser beams," *Opt. Commun.*, vol. 429, pp. 175–179, Dec. 2018.

[4] M. Ibrahim, "17 years of ranging from the helwan SLR station," *Astrophys. Space Sci.*, vol. 335, no. 2, pp. 379–387, Oct. 2011.

[5] Z. Liang, X. Dong, M. Ibrahim, Q. Song, X. Han, C. Liu, H. Zhang, and G. Zhao, "Tracking the space debris from the changchun observatory," *Astrophys. Space Sci.*, vol. 364, no. 11, p. 201, Nov. 2019.

[6] D. L. Song, J. Chang, Y. F. Zhao, and Z. X. Zhang, "Anti-detection technology of cat eye target based on decentered field lens," *Chin. Phys.*, vol. 09, no. 27, pp. 337–341, Sep. 2018.

[7] M. J. Khan, H. S. Khan, Y. Adeel, K. Khurram, and A. Asad, "Modern trends in hyperspectral image analysis: A review," *IEEE Access*, vol. 14, pp. 118–129, 2018.

[8] G. W. Paterson, R. J. Lamb, R. Ballabriga, D. Maneuski, V. O'Shea, and D. McGrouther, "Sub-100 nanosecond temporally resolved imaging with the Medipix$_3$ direct electron detector," *Ultramicroscopy*, vol. 210, Mar. 2020, Art. no. 112917.

[9] Y. C. Lin, C. J. Cheng, and L. C. Lin, "Tunable time-resolved tick-tock pulsed digital holographic microscopy for ultrafast events," *Opt. Lett.*, vol. 11, no. 42, pp. 82–85, Nov. 2017.

[10] X. D. Li and S. J. Song, "Stabilization of delay systems: Delay-dependent impulsive control," *IEEE Trans. Autom. Control*, no. 62, pp. 406–411, Jul. 2017.

[11] R. W. Rui, "Effect of gate width of laser range gating imaging on image SNR," *Chin. Opt.*, vol. 8, no. 6, pp. 951–956, 2015.

[12] J. Y. Hu, C. Q. Pei, J. S. Tian, J. F. Wang, Y. M. Fang, and W. L. Wen, "Design and experimental study of ICCD gated pulse source," *Acta Photon. Sinica*, vol. 47, no. 9, Sep. 2018, Art. no. 911001.

[13] W. Ren, J. E. Guan, J. H. Liu, J, Y. Chen, X. S. Feng, "Range-gated imaging in turbid conditions using a combination of intensity and polarization information," *Phys. Scripta*, vol. 94, no. 10, pp. 105–505, Jun. 2019.

[14] L. Sun, X. W. Wang, X. Q. Liu, P. S. Lei, J. He, S. T. Fan, Y. Zhou, and Y. L. Liu, "Lower-upper-threshold correlation for underwater range-gated imaging self-adaptive enhancement," *Appl. Opt.*, vol. 55, no. 29, pp. 8248–8255, Oct. 2016.

[15] P. Rosendahl, K. Plak, A. Jacobi, M. Kraeter, N. Toepfner, O. Otto, C. Herold, M. Winzi, M. Herbig, Y. Ge, S. Girardo, K. Wagner, B. Baum, and J. Guck, "Real-time fluorescence and deformability cytometry," *Nature Methods*, vol. 15, no. 5, pp. 355–358, May 2018.

[16] H. Tian, J.-P. Zhu, S.-W. Tan, J.-J. Tian, Y.-Y. Zhang, and X. Hou, "Polarization-based range-gated imaging in birefringent medium: Effect of size parameter," *Chin. Phys. B*, vol. 27, no. 12, Dec. 2018, Art. no. 124203.

[17] V. Kabashnikov and B. Kuntsevich, "Distance determination based on the delay time-intensity profile analysis in range-gated imaging," *Appl. Opt.*, vol. 56, no. 30, pp. 8378–8384, Oct. 2017.

[18] W. Xinwei, L. Youfu, and Z. Yan, "Multi-pulse time delay integration method for flexible 3D super-resolution range-gated imaging," *Opt. Express*, vol. 23, no. 6, p. 7820, Mar. 2015.

[19] D. Z. Lu, X. W. Wang, S. T. Fan, J. He, Y. Zhou, and Y. L. Liu, "Ns-scaled time-coding method for real-time 3D super-resolution range-gated imaging," *Chin. Opt. Lett.*, vol. 13, no. 08, pp. 81–102, Aug. 2015.

[20] Y. Mu, H. Fan, C. Liu, and G. Liu, "A waveguide gate-type complex detecting mechanism on micro-channel plate substrate," *Chin. J. Electron.*, vol. 28, no. 3, pp. 625–629, May 2019.
[21] Y. Xu, T. Xu, H. Liu, H. Cai, and C. Wang, "Gain regulation of the microchannel plate system," *Int. J. Mass Spectrometry*, vol. 421, pp. 234–237, Oct. 2017.
[22] Q. G. Hu and Y. N. Mu, "The influence of vibration on spatial coupler and the tapered receiver," *J. Phys. Commun.*, vol. 02, no. 03, pp. 18–35, Feb. 2018.
[23] N. Shivaram, E. G. Champenois, J. P. Cryan, T. Wright, T. Wingard, and A. Belkacem, "Focal overlap gating in velocity map imaging to achieve high signal-to-noise ratio in photo-ion pump-probe experiments," *Appl. Phys. Lett.*, vol. 109, no. 25, pp. 101–254, Aug. 2016.
[24] A. McIlvenny, D. Doria, L. Romagnani, H. Ahmed, P. Martin, S. D. R. WIlliamson, E. J. Ditter, O. Ettlinger, G. S. Hicks, P. McKenna, Z. Najmudin, D. Neely, S. Kar, and M. Borghesi, "Absolute calibration of microchannel plate detector for carbon ions up to 250 MeV," *J. Instrum.*, vol. 14, no. 4, Apr. 2019, Art. no. C04002.
[25] X. Hui, D. Yu, X. Song, W. Wang, J. Liu, X. Li, Y. Zhang, W. Xi, X. Yuan, X. Zhu, and B. Ding, "Radial position sensitive microchannel plate detector with ring-strip resistive anode and integrated electronics," *J. Instrum.*, vol. 13, no. 9, Sep. 2018, Art. no. T09004.
[26] P. N. Huang, G. P. Dong, and M. Q. Pan, "The velocity distribution of a cutting microchannel plate based on the resistance network method," *Chem. Eng. Sci.*, vol. 208, no. 23, pp. 115–140, Nov. 2019.
[27] J. Wang, J. Xie, L. Xia, H. Zhao, K. Byrum, M. Demarteau, R. Dharmapalan, J. W. Elam, A. U. Mane, E. May, R. Wagner, and D. Walters, "Design improvement and bias voltage optimization of glass-body microchannel plate picosecond photodetector," *IEEE Trans. Nucl. Sci.*, vol. 64, no. 7, pp. 1871–1879, Jul. 2017.
[28] Z. Y. Zhang, D. Y. Yu, J. L. Liu, L. P. Yang, W. Wang, X. X. Li, X. N. Zhu, X. X. Song, X. F. Hui, W. Xi, X. Li, H. P. Liu, and X. H. Cai, "A two-dimensional position-sensitive microchannel plate detector realized with two independent one-dimensional resistive anodes," *Rev. Sci. Instrum.*, vol. 89, no. 7, p. 73302, Jul. 2018.
[29] W. Cao, B. Zhu, X. Bai, P. Xu, B. Wang, J. Qin, Y. Gou, F. Lei, B. Liu, J. Guo, J. Zhu, and Y. Bai, "High-sensitivity and long-life microchannel plate processed by atomic layer deposition," *Nanosc. Res. Lett.*, vol. 14, no. 1, p. 153, Dec. 2019.
[30] V. Ivanov, A. Barnyakov, M. Barnyakov, and I. Ovtin, "Numerical simulation of fast photo detectors based on microchannel plates," *J. Instrum.*, vol. 12, no. 9, pp. 9–24, Sep. 2017.
[31] K. Saha, R. Benmaimon, A. Prabhakaran, M. L. Rappaport, O. Heber, D. Schwalm, and D. Zajfman, "Position information by signal analysis in real time from resistive anode microchannel plate detector," *J. Instrum.*, vol. 11, no. 7, Jul. 2016, Art. no. T07006.

YINING MU was born in 1985. He is currently a Full Professor working with the Faculty of Science, Changchun University of Science and Technology. He is a Top innovative talents in Jilin. His research interests include photoelectric devices and systems. He was separately granted award for scientific and technological advancement in Jilin.

FANQI TANG was born in 1995. He is currently pursuing the Ph.D. degree with the Department of Electronic Science and Technology, Faculty of Science, Changchun University of Science and Technology. His main research interests include infrared technology and systems.

MAKRAM IBRAHIM was born in 1963. He received the Dr.Eng. degree from Hokkaido University, Japan. He is currently a Professor and the Head of the Solar and Space Research Department, National Research Institute of Astronomy and Geophysics (NRIAG), Egypt. His research interests include satellite and laser ranging, space physics, and optics.

YAN ZHU is currently pursuing the Ph.D. degree with the Department of Electronic Science and Technology, Faculty of Science, Changchun University of Science and Technology. His main research interests include white optical communication systems and optoelectronic devices.

WENXIN LIU is currently pursuing the M.S. degree in optoelectronic information science and engineering with the Faculty of Science, Changchun University of Science and Technology. Her main research interests include photoelectronic device design and integrated circuit design technology.

ZHE CAO is currently pursuing the M.S. degree in electronic science and technology with the Faculty of Science, Changchun University of Science and Technology. His main research interests include photoelectronic device design and integrated circuit design.

TIANQI CHEN is currently pursuing the M.S. degree in optoelectronic information science and engineering with the Faculty of Science, Changchun University of Science and Technology. His research interests include optical communication and optoelectronic devices.